Indian Journal of Chemistry
Vol. 63, July 2024, pp. 716-726
DOI: 10.56042/ijc.v63i7.8354

Synthesis and characterization of new niacinamide compounds and computational and experimental investigation of their anticancer and antibacterial activity

Haşim Ertek & Koray Sayın*

Department of Chemistry, Faculty of Science, Sivas Cumhuriyet University, Sivas, Türkiye

E-mail: krysayin@gmail.com

Received 27 January 2024; accepted (revised) 28 June 2024

4-Niacinamide compounds have been synthesized and characterized. These compounds have been optimized at B3LYP-D3/6-311++G(d,p) level in water. The electronic properties of these have been investigated by employing contour plot of frontier molecular orbitals, molecular electrostatic potential map and Fukui plot. Cell viability test have been carried out against colon, breast and gastric adenocarcinoma. Of the compounds studied, only NIA1 and NIA2 are found to be effective against stomach cancer. Molecular docking calculations against epidermal growth factor receptor and thymidine kinase have also been performed by *in silico* analysis. MM-GBSA analyses have been performed and binding energies between ligand and receptor have been calculated. Finally, ADME and pharmacophore analyses of the newly synthesized molecules have been performed. After considering all the results, it is observed that both experimental and computational results of NIA1 and NIA2 are in agreement with each other, with NIA1 showing better results than NIA2.

Keywords: DFT, Synthesis, Niacinamide, Anticancer, Antibacterial

Health is one of the most important issues for living beings today, and if there is the slightest problem in the health of a living being, this can greatly affect the welfare level of the living being. For this aim, many researchs have been doing by many researchers which their fields are different from each other. For computational and synthesis chemists, the focus is on screening and synthesising new chemicals that can improve welfare. However, the health problem is not unique in this respect. Today, there are many health problems such as cancer, fungi, bacteria, *etc*. Each subject needs to be focussed separately and research is progressing in this way today. Cancer is the second leading cause of the death. According to World Health Organization (WHO) data, approximately 10 million people are known to have died of cancer in 2020 (Ref. 1). Additionally, the most common detected cancers are breast, lung, colon, rectum, and prostate[2-4]. However, this situation is different when analysed in terms of mortality rates. To prevent cancer prolifaration and effect, many chemicals have been synthesized and completed of their *in silico*, *in vitro* and *in vivo* studies[5-10]. Although niacinamide derivative compounds are mostly used in cosmetic studies and skin problems, it has been emphasised in many studies that niacinamide-derived compounds exhibit anticancer properties in recent years and related articles have been published[11-13]. It is also reported that these compounds have antimicrobial effects. Because these compounds have a pyridine nitrogen, carbonyl group and amine nitrogen. These groups are among the most likely groups to interact with the target protein.

In this study, new niacinamide compounds are synthesized and characterized by spectral techniques which are ^{1}H and ^{13}C NMR, IR, and LC-QTOF-MS. Then, these compounds are fully optimized at B3LYP-D3/6-311++G(d,p) level in water. In this stage, the Polarizable Continuum Model (PCM) using the integral equation formalism variant (IEF-PCM) is selected as solvation model to consider the solute-solvent interactions. Experimental spectral results which are ^{1}H and ^{13}C NMR, and IR, are verified with computational results. As for the anticancer activity, cell proliferation test is performed against 3 cancer cell lines which are human breast cancer [MCF-7 (HTB-22)], human colon cancer [HT-29 (HTB-38)] and human gastric cancer [SNU1 (CRL-5971)] *via* XTT test. Additionally, obtained resuts in *in vitro* are supported by *in silico* analyses. *In silico* analyses, molecular docking, ADME, pharmacophore calculations and molecular dynamic calculations were done in detail. By *in silico* calculations, anticancer and antibacterial properties are investigated. The

target proteins for anticancer and antibacterial studies are selected as 7JXQ[14] and 4QGG[15], respectively. NIA1 is found as the best compound in this study both experimentally and *in silico* analyses.

Experimental Section

Reagents

2-Chloronicotinoyl chloride, 6-chloronicotinoyl chloride, 4-chloro-2-fluoroaniline, 2-bromo-5-fluoro-aniline, 5-amino-2-fluorobenzonitrile, trimethylamine (TEA) and solvents which are methanol (MeOH), 1,2-dichloroethane (1,2-DCE), chloroform, petroleum ether, diethyl ether, DMSO was purchased from Merck kGaA.

Instrumentation

IR spectra (4000–400 cm^{-1}) were obtained using IR spectra (ATR) and recorded on a Bruker Tensor II FT-IR spectrometer. ^1H and ^{13}C NMR spectra were recorded on a JEOL (400MHz) JNM-ECZ400S/L1 NMR instrument in DMSO-d_6 at RT; δ in ppm relative to tetramethylsilane (TMS), with J in Hertz (Hz). Agilent Technology Inc. of 1260 Infinity HPLC System was coupled with 6530 Q-TOF LC/MS detector and ZORBAX SB-C18 (2.1×50mm, 1.8 μm) column. ^1H and ^{13}C NMR, and LC-QTOF-MS analyses of the compounds were carried out at Sivas Cumhuriyet University.

Synthesis of compounds

Related niacinamide derivatives were synthesized according to Fig. 1. Related aniline derivatives are added to the solution of 6-chloronicotinoyl chloride in DCM:1,2-DCE (1:1) with trimethylamine. The mixture were refluxed nearly 3 h and extracted with CH_2Cl_2 three times. The organic part was dried over anhyd. Na_2SO_4 and the solvent evaporated. The residue was crystallized in methanol/DCM (3:1). This synthesis route has been used by Taşkın Kafa *et al*. 2022 (Ref. 16).

The synthesized compounds were characterized by spectral characterization techniques, IR, ^1H and ^{13}C NMR, and LC-QTOF-MS. The related spectra are given in Supplementary Information. The obtained results are given as follow for each compound.

2-Chloro-N-(4-chloro-2-fluorophenyl)niacinamide, NIA1: Yield 81%. Powder, pink crystals. IR: 3218, 3176, 1660, 1582, 1520, 1491, 1401, 1308, 1199, 1118, 1065, 901.8, 851.5, 815.1, 734, 700.3, 552.6, 414 cm^{-1}; ^1H NMR (400 MHz, DMSO-d_6): δ 10.57, 8.48 (dd, J = 4.8, 1.8 Hz, 1H), 8.02 (dd, J = 7.6, 1.9 Hz, 1H), 7.90 (t, J = 8.5 Hz, 1H), 7.54 – 7.46 (m, 2H), 7.29 (d, J = 8.7 Hz, 1H); ^{13}C NMR (101 MHz, DMSO-d_6): δ 164.63, 155.85, 153.35, 151.17, 147.01, 138.85, 133.09, 129.96 (d, J = 9.6 Hz), 126.39 – 126.34 (m), 125.45 – 124.86 (m), 123.61, 117.00 (d, J = 23.3 Hz); HPLC-TOF/MS: m/z 282.9847 ($[M-H]^-$, $C_{12}H_6Cl_2FN_2O^-$; Calcd 282.98467).

6-Chloro-N-(4-chloro-2-fluorophenyl)niacinamide, NIA2: Yield 39.5%. White powder. IR: 3287, 3096, 3054, 1654, 1597, 1530, 1489, 1406, 1324, 1194, 1132, 1075, 1019, 899.4, 855.7, 829.7, 746.2, 655.9, 562.9, 532, 469.4 cm^{-1}; ^1H NMR (400 MHz, DMSO-d_6): δ 10.44, 8.93 – 8.86 (m, 1H), 8.29 (dd, J = 8.3, 2.4 Hz, 1H), 7.73 – 7.60 (m, 2H), 7.54 – 7.42 (m, 1H), 7.28 (d, J = 8.6 Hz, 1H); ^{13}C NMR (101 MHz, DMSO-d_6): δ 163.66, 157.10, 154.60, 153.67, 149.99, 139.71, 130.81 (d, J = 9.9 Hz), 129.39, 128.29 (d, J = 2.5 Hz), 125.33 – 124.88 (m), 124.77, 117.12 (d, J = 23.7 Hz); HPLC-TOF/MS: m/z 282.9843 ($[M-H]^-$, $C_{12}H_6Cl_2FN_2O^-$; Calcd 282.98467).

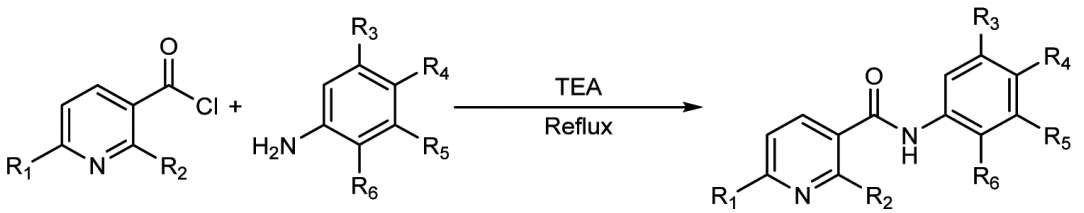

Assignment	R_1	R_2	R_3	R_4	R_5	R_6
NIA1	H	Cl	H	Cl	H	F
NIA2	Cl	H	H	Cl	H	F
NIA3	Cl	H	F	H	H	Br
NIA4	Cl	H	H	F	CN	H

Fig. 1 — Synthetic scheme of the studied compounds

N-(2-Bromo-5-florophenyl)-6-chloroniacinamide, NIA3: Yield 54%. Off-white powder. IR: 3285, 3095, 1646, 1584, 1527, 1455, 1420, 1282, 1262, 1164, 1131, 1097, 1030, 977, 850.1, 801.6, 758.9, 626.1, 596.2, 583.3, 536.3 cm^{-1}; ^1H NMR (400 MHz, DMSO-d_6): δ 10.38, 8.92 (dd, J = 2.6, 0.8 Hz, 1H), 8.31 (dd, J = 8.3, 2.5 Hz, 1H), 7.72 (dd, J = 9.0, 5.9 Hz, 1H), 7.68 (dd, J = 8.3, 0.7 Hz, 1H), 7.49 (dd, J = 9.9, 3.1 Hz, 1H), 7.12 (ddd, J = 8.9, 8.1, 3.1 Hz, 1H); ^{13}C NMR (101 MHz, DMSO-d_6): δ 163.62, 162.83, 160.39, 153.78, 149.90, 139.63, 137.95, 137.83, 134.51, 134.42, 129.39, 124.91; HPLC-TOF/MS: *m/z* 328.9336 ($[M-H]^-$, $C_{12}H_6BrClFN_2O^-$; Calcd 328.932).

6-Chloro-N-(3-cyano-4-florophenyl)nicotinamide, B: Yield 49%. Light brown powder. IR: 3330, 3067, 2240, 2115, 1625, 1680, 1583, 1552, 1503, 1456, 1401, 1257, 1219, 1132, 1110, 1018, 882.2, 834,.4, 735.5, 658.7, 533.4, 587.4, 465 cm^{-1}; ^1H NMR (400 MHz, DMSO-d_6): δ 10.72, 8.87 (d, J = 2.5 Hz, 1H), 8.27 (dd, J = 8.3, 2.5 Hz, 1H), 8.17 (dd, J = 5.8, 2.7 Hz, 1H), 7.96 (ddd, J = 9.2, 4.9, 2.7 Hz, 1H), 7.66 (dd, J = 8.3, 0.7 Hz, 1H), 7.49 (td, J = 9.1, 0.7 Hz, 1H); ^{13}C NMR (101 MHz, DMSO-d_6): δ 163.71, 160.38, 157.87, 153.71, 149.87, 139.57, 136.25 (d, J = 3.8 Hz), 129.70, 128.20 (d, J = 9.2 Hz), 124.77, 117.64 (d, J = 20.9 Hz), 114.38, 100.47 (d, J = 16.6 Hz); HPLC-TOF/MS: *m/z* 274.0200 ($[M-H]^-$, $C_{13}H_6ClFN_3O^-$; Calcd 274.019).

Computational Chemistry

Gaussian software was used in the computational investigations[17,18]. The synthesized compounds were fully-optimized at the B3LYP-D3 method with 6-311++G(d,p) basis set in water. In this stage, the polarizable continuum model (PCM) using the integral equation formalism variant (IEF-PCM) was used as solvent model to considere solute-solvent interactions. No imaginary frequency was observed in IR spectrum. IR, ^1H NMR and ^{13}C NMR spectrum were calculated at the same level of theory. Additionally, electronic properties of these compounds were investigated *via* contour plots of frontier molecular orbitals (FMOs) and moleculer electrostatic potential (MEP) map. Finally, Fukui functions were calculated for studied compounds using Maestro 12.8 software[19].

Cell Culture Studies

MCF7 (HTB-22/human breast cancer), HT29 (HTB-28/colon cancer), and SNU1 (CRL-5971/gastric cancer) obtained from the American Type Culture Collection (ATCC, Manassas, VA, USA) cell lines were used. Cells were cultured in 25 cm^2 flasks containing RPMI containing 10% Fetal Bovine Serum (FBS), 1% penicillin/ streptomycin, and 1% L-glutamine. Cells were maintained at 37°C in a humidified atmosphere with 5% CO_2. Cells reaching 80% density were passaged. Cells were seeded on a 96-well plate with the number of cells in each well of 1×10^4 cells. The new synthesis compounds were dissolved in DMSO and diluted in culture medium before processing with a final DMSO content of 5%.

Cell Viability Assay

MCF7, HT29, and SNU1 cell lines were used to evaluate the anticancer activity of nine newly synthesized compounds. The XTT colorimetric method (2,3-bis-(2-methoxy-4-nitro-5-sulphophenyl)-5-[(phenylamino)carbonyl] -2H-tetrazolium hydroxide) (Biological Industries) was used to assess cell viability. MCF7, HT29, and SNU1 cells in growth phase were seeded at a density of 1×10^4 cells per well in 96-well microplates prepared in RPMI 1640 culture medium (100-µL).

Processing was started after 24 h of incubation. Synthesis compounds were administered to all cell lines individually at a dose of 40 µM. Cells were classified as control group and drug group. No drug was administered to the control group. The prepared 96-well plate was kept in the incubator and removed after 24 h. Wells were washed with phosphate buffered saline (PBS). Then, 100 µL of phenol red-free DMEM and 50 µL of XTT solution were added to all wells and the plates were kept at 37°C for 4 h. Absorbance values were determined at 450 nm using an ELISA microplate reader (Thermo Fisher Scientific, Altrincham, UK). This procedure was repeated three times. Cell viability was accepted as 100% in the control group. Cell viability was calculated using the formula (%Cell viability = (Concentration O.D./Control O.D.)×100).

In silico Analysis

Anticancer and antibacterial properties of synthesized new niacinamides were examined *via in silico* analyses. To predict the anticancer activity of related compounds, epidermal growth factor receptor (EGFR) was selected due to the fact that it was known as a co-target for stomach cancer, breast cancer, prostate cancer, non-small cell lung cancer, and colon

cancer[20]. EGFR was expressed in many tissues and plays significant roles in many cellular processes that are vital for survival and cell growth. EGFR protein was taken from the protein data bank web tool as 7JXQ. As for the antibacterial activity, thymidine kinase (TMK) in *Staphylococcus aureus* was selected as target. TMK is significant for cells engaged in active DNA synthesis and is organized by feedback control mechanism. Furthermore, TMK play important role in the converting of dTMP to dTDP and TMK have been characterized in many bacteria and eukaryotes. 4QGG was selected as target protein for molecular docking calculations.

Molecular Docking Calculations

Selected proteins which are 7JXQ and 4QGG were prepared to docking calculations using "Protein Preparation"[21] module. Additionally, synthesized niacinamide derivatives were prepared using "LigPrep" module[22]. In these preparations, *p*H was defined as 7±2. Then, x/y/z coordinates of receptor binding domain (RBD) for 7JXQ and 4QGG was defined using "Receptor Grid Generation" module as 18.19/-30.6/-20.63 and 20.45/-0.15/-10.44, respectively. All docking calculations were performed using "Ligand Docking" module[23] in Maestro 12.8 software.

ADME Calculations

ADME properties of chemicals could give significant clues in the pharmacophore characteristics and were calculated using "Ligand-Based ADME/Tox Prediction" module at Maestro 12.8 software[24]. QikProp parameters were calculated and compared with their references.

Pharmacophore Map

Pharmacophore model were calculated using "Develop Pharmacophore Model" module in Maestro 12.8 (Ref. 25). In calculations Multiple ligands section was selected to find best alignment and common features.

Molecular mechanics with generalised Born and surface area solvation (MM/GBSA) calculations

To calculated binding energy between ligand and target protein, MM/GBSA calculations were performed. MM/ GBSA analyses were started after the docking calculations were finished. These calculations were performed using the complex structures obtained as a result of docking calculations and the "MM/GBSA" module in Maestro 12.8 software was used.

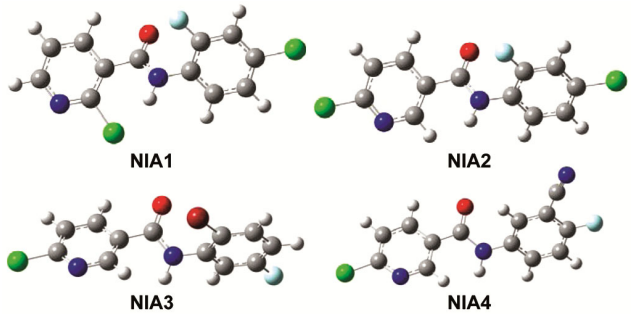

Fig. 2 — The optimized structure of examined niacinamide derivatives

Results and Discussion

Full-Optimization

The synthesized compounds are optimized at B3LYP-D3/6-311++G(d,p) level in the water. The ground state structure of these compounds are showed in Fig. 2.

According to Fig. 2, non-planar structure is dominant for each studied compound. In the structures, two benzene rings are observed to be at positions almost 90 degrees to each other. No imaginary frequency is observed in IR spectrum. So, calculated structure is stable and belong to ground state level.

IR Spectra

IR spectrum is an essential spectral technique for the characterization of synthesized compounds. Functional groups can be determined using this spectral technique. IR-ATR spectrum of synthesized compounds are obtained both experimentally and computationally. Stretching frequency of some functional groups such as C=O, NH, *etc*. are reported as follow. Stretching frequency of –NH bond is observed in the range of 3218 – 3330 cm^{-1} while it is calculated in the range of 3592 – 3628 cm^{-1}. Vibrational frequency of carbonyl group is observed in the range of 1640 – 1680 cm^{-1} while it is calculated in the range of 1683 – 1695 cm^{-1}. Stretching frequency for C-F bond is calculated nearly 1228 – 1304 cm^{-1} whilst it is observed nearly 1199 – 1285 cm^{-1} as experimentally. As for the C-Cl and C-Br bonds, it is observed ~850 and 596 cm^{-1}, respectively. IR frequency of these bonds is calculated nearly 825 and 590 cm^{-1}, respectively. Finally, stretching frequency of nitrile group is observed nearly 2240 cm^{-1}. It is calculated as 2313 cm^{-1}. As can be easily understood, it is clearly seen that the experimental and computational results support each other and are in agreement with each other.

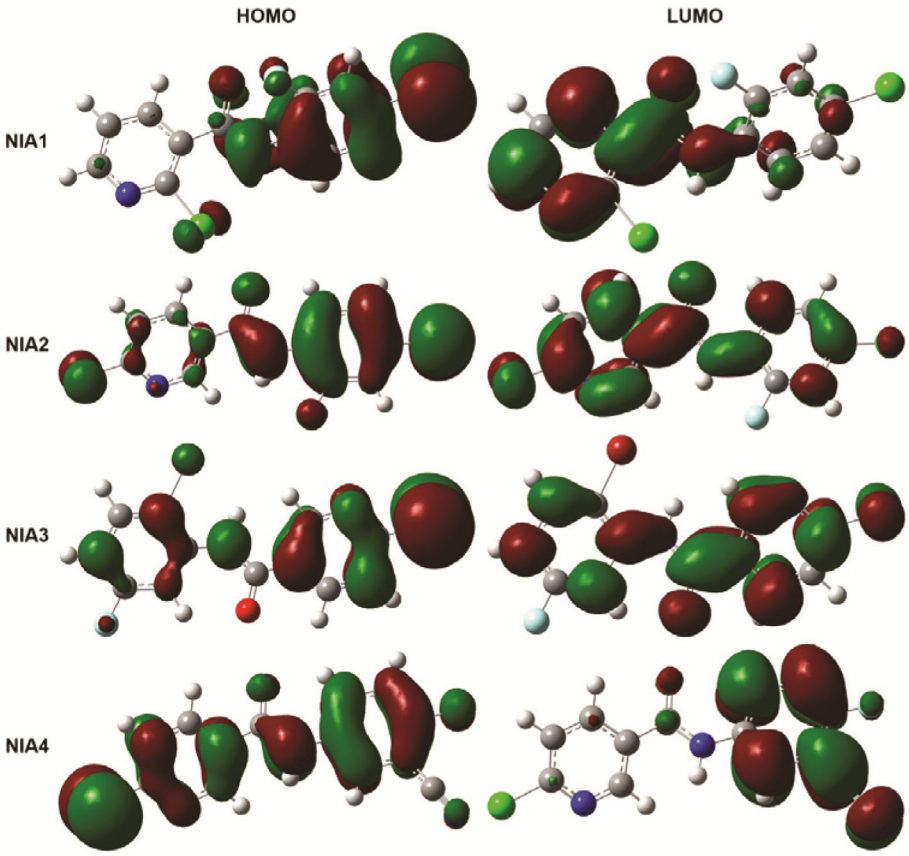

Fig. 3 — Contour plot of FMOs of synthesized compounds.

NMR Spectra

^{1}H NMR and ^{13}C NMR spectrum is so significant technique to characterize the newly synthesized. In this section, experimental results are examined in detail. Additionally, ^{1}H NMR and ^{13}C NMR spectrum are calculated at mentioned calculation level. Experimental and calculated results are compared with each other. Chemical shift value of NH proton is observed nearly 10.4 ppm and this one is calculated as nearly 8.5 ppm. Chemical shift value of carbon atom in carbonyl group is observed nearly 164 ppm whilst it is calculated nearly 161 ppm. Finally, chemical shift values of carbon atom (CN) in NIA4 is 114.4 ppm and it is calculated as 112.1 ppm.

Electronic Properties

Contour plot of FMOs

Frontier molecular orbitals, HOMO and LUMO, are significant and give important clues about the reactive site on molecule. Contour plot of HOMO and LUMO are calculated and represented in Fig. 3.

There are two electrons on HOMO and delocalization region of them can be seen easily from contour plot of HOMO. It is seen that the electron is delocalised on all atoms in the molecule. This indicates that the molecule can easily interact through these regions. As for the LUMO plots, it means that the electrons of the opposite type that can interact are more likely to interact with the regions where the lobes are located. In particular, it is clearly observed that benzene rings are the most favourable group for interaction.

MEP maps

Electronic properties of synthesized compounds can be investigated using molecular electrostatic potential (MEP) maps. This illustration is calculated for each compound and represented in Fig. 4. Additionally, in order to facilitate the interpretation of the map, the electron density chart is added to the Fig. 4.

According to Fig. 4, there are various colors on the molecular surface. These colours form according to

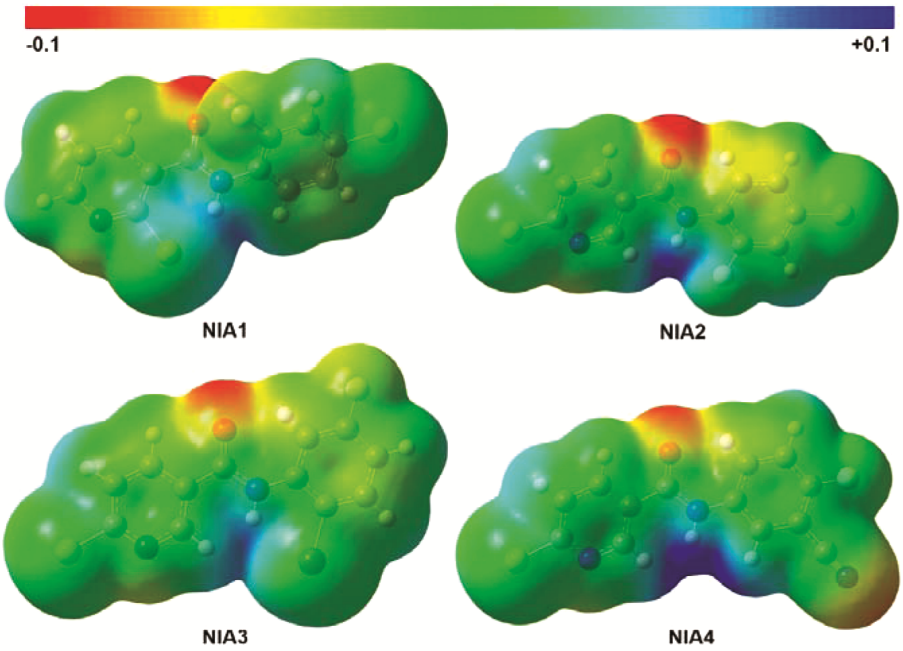

Fig. 4 — MEP maps of studied molecules

electron density of the surface. The electron-dense region is shown in red, while the electron-weakest region is shown in dark blue. According to these regions, red color is only dominant on the environment of the oxygen atom. Generally, there is green on mainly surface of molecules. When the molecules are compared with each other, it can be said that the molecule in which red and yellow are more dominant can interact more easily. In this case, it can be said that NIA1 and NIA3 can enter the interaction most easily. It is observed that yellow colours are more dominant around the benzene ring.

Fukui Functions

Determination and comparison of electrophilic and nucleophilic active sites is very important in predicting biological activity and comparing molecules with each other. For this purpose, electrophilic active sites (f^-) and nucleophilic active (f^+) sites defined as Fukui function were calculated and visualised. They are represented in Fig. 5.

According to Fig. 5, there are red and blue balloons on the environment of the atoms on the studied compound. Nucleophilic active sites is seen as around the the pyridine ring for each compound. This ring has electrons and can attach the nucleophile easily. As for the electrophilic active site, the blue and red balloons appear to be mostly on the benzene ring and carbonyl. These regions seem to be suitable for electrophilic attack.

***In vitro* Cytotoxicity Analysis**

Cell viability assay is significant analysis for the determining of cell proliferation. 3 cancer cell lines which are human breast cancer (MCF-7), human colon cancer (HT-29) and human gastric cancer (SNU1) cell lines are used in this study. The anticancer activities of newly synthesized compounds are investigated. In the first step, all compounds were applied to 3 cell lines at different consantrations which are 0.001, 0.01, 0.1, 1, 10, 25, 50 and 100 µM. Cell viability percentages were calculated by XTT colorimetric method 24 h after the application. Each concentration study was designed and implemented with 3 repetitions. Then, the averages of the results were calculated. Experimentally obtained cell viability test results are given in Table 1.

According to Table 1, it is observed that the molecules studied were not effective against colon and breast cancer. However, it is determined that some molecules are effective against gastric cancer and some of them are not effective in the desired concentration range. It is observed that NIA1 and NIA2 were effective against gastric cancer. IC_{50} values are calculated as 7.22 and 28.28 µM, respectively, using AAT Bioquest web tool. The best

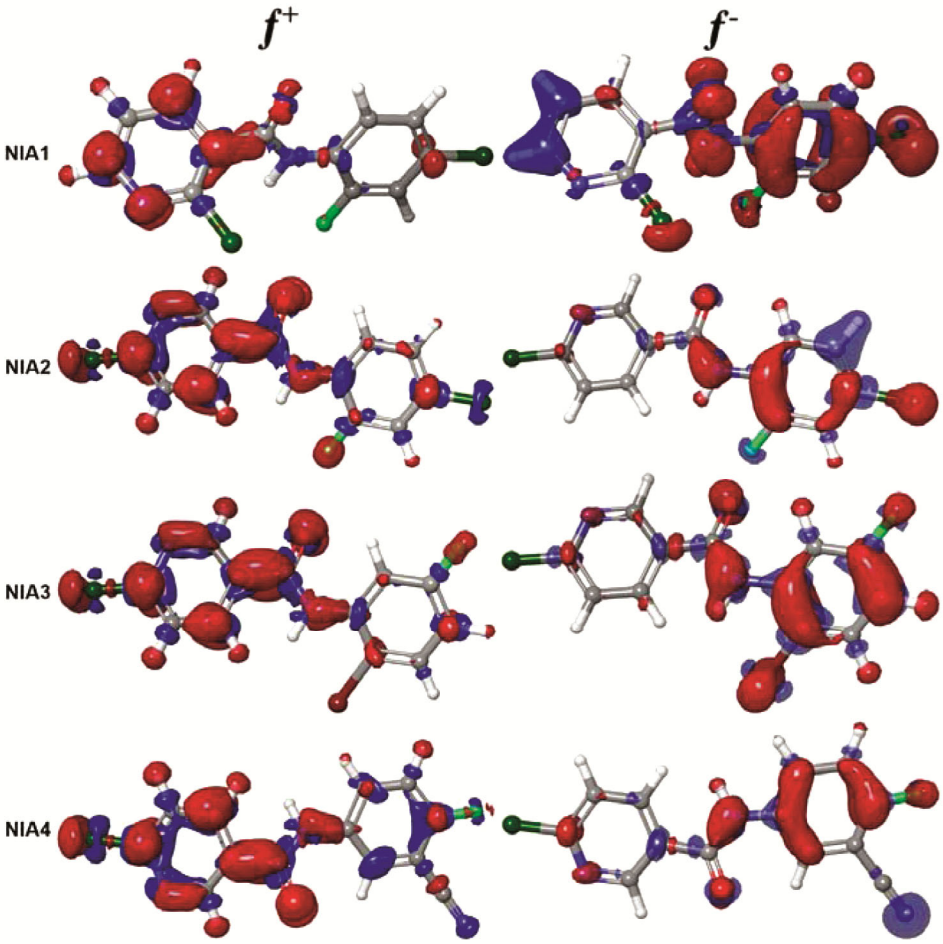

Fig. 5 — Fukui plots of studied molecules

resuls is obtained in NIA1 against SNU1, gastric adenocarsinamo cell line.

In silico Analyses

Molecular Docking

Synthesized molecules are prepared at *p*H=7±2 and the target proteins, 7JXQ and 4QGG are prepared at OPLS4 method. Epidermal growth factor receptor (EGFR) play important role in the growth of gastric cancer line. 7JXQ is the EGFR protein. The inhibition properties of studied compounds are investigated to determine the anticancer properties. Furthermore, 4QGG is selected for the thymidine kinase (TMK) in *Staphylococcus aureus* to investigate the antibacterial properties. Molecular docking results, docking score (DS), van der Walls interaction energy (E_{vdW}), Coulomb interaction energy (E_{Coul}), and total interaction energy (E_{Total}) are given in Table 2.

According to Table 2, it is calculated that NIA1 of EGFR inhibition properties is the best. It's docking score is -6.906 and this one is good for inhibitör candidates. This value implies the harmony between inhibitor and receptor. As for the interaction energies, total interaction enegy of NIA1 and NIA2 is close to each other. In general, the best result is obtained in NIA1, and although the docking score is not as good as that of NIA1, it is seen that NIA2 is effective according to the total interaction energy. The results obtained in molecular docking calculations are in agreement with the XTT results. As for the antibacterial properties, it is seen that the results obtained against 4QGG are close to each other, both the doking score and the total interaction energies are close to each other. In this case, it is seen that these molecules exhibit antibacterial properties and the results to be obtained are close to each other.

Table 1 — Percentage of cell viability assay of studied compound at different concentration (μM)

	NIA1 (7.22)			NIA2 (28.28)		
Concentration	HT-29	MCF-7	SNU-1	HT-29	MCF-7	SNU-1
100	>100	86	39	78	79	45
50	>100	>100	43	75	88	50
25	>100	>100	52	80	>100	50
10	>100	>100	56	90	>100	55
1	>100	>100	58	>100	>100	62
0.1	>100	>100	56	>100	>100	60
0.01	>100	>100	85	>100	>100	85
0.001	>100	>100	91	>100	>100	87
	NIA3			NIA4		
Concentration	HT-29	MCF-7	SNU-1	HT-29	MCF-7	SNU-1
100	>100	>100	80.1	86.9	75.8	93.8
50	>100	>100	85.3	78	96.6	90.1
25	>100	>100	85.1	83	>100	82.3
10	>100	>100	99.5	88.7	>100	81.5
1	>100	>100	95.1	96.8	>100	84.9
0.1	>100	>100	83.6	85.1	>100	84.0
0.01	>100	>100	96.7	91.3	>100	94.9
0.001	>100	>100	91.6	85.9	>100	69.2

Table 2 — The molecular docking results

Assignment	DS[a]	E_{vdW}[a]	E_{Coul}[a]	E_{Total}[a]
	For 7JXQ			
NIA1	–6.906	–31.114	–3.419	–34.533
NIA2	–2.939	–29.960	–4.590	–34.550
NIA3	–2.262	–29.357	–4.099	–33.455
NIA4	–2.174	–26.123	–2.994	–29.117
	For 4QGG			
NIA1	–3.370	–23.596	–0.349	–23.945
NIA2	–3.752	–25.155	–0.743	–25.898
NIA3	–3.264	–24.379	–1.034	–25.413
NIA4	–3.331	–26.233	–1.317	–27.550

[a] in kcal/mol

MM-GBSA

MM-GBSA calculations is so important to determine the binding energy between ligand and receptor. To be obtained energy is different from the total interaction energy. Maestro 12.8 program was used to calculate the binding energy for the calculated complex structures (doking structure). Calculated complex energy ($E_{Complex}$), receptor energy ($E_{Receptor}$), ligand energy (E_{Ligand}), and binding energy ($E_{Binding}$) are given in Table 3.

According to Table 3, the better binding energy is obtained in NIA1 and NIA2 for 7JXQ nearly -45 kcal/mol. This value is better than those of NIA3 and NIA4. So, inhibition properties of NIA1 and NIA2 is better than those of NIA3 and NIA4. In MM-GBSA calculation of 4QGG, binding energies are close to each other. This result implies that the antibacterial properties of the molecules will be close to each other. The results obtained in MM-GBSA are in agreement with the molecular docking results.

ADME

ADME properties of studied compounds are significant to determine the pharmacokinetics properties. ADME calculations are performed for studied compounds. Some parameters are given in Table 4 to evaluate the pharmacokinetic properties of synthesized compounds.

According to Table 4, when the calculated Qik parameters are compared with the reference results, it can be said that they are in general agreement. In the relevant table, the parameters that do not comply with

Table 3 — MM-GBSA results

Assignment	$E_{Complex}$[a]	$E_{Receptor}$[a]	E_{Ligand}[a]	$E_{Binding}$[a]
		For 7JXQ		
NIA1	–11952.923	–11901.347	–5.893	–45.683
NIA2	–11956.249	–11901.347	–5.180	–44.250
NIA3	–11957.805	–11901.347	–16.570	–35.203
NIA4	–11949.479	–11901.347	–12.929	–32.658
		For 4QGG		
NIA1	–7876.382	–7834.689	–5.906	–35.787
NIA2	–7878.899	–7834.689	–6.268	–37.942
NIA3	–7892.440	–7834.689	–18.128	–39.622
NIA4	–7884.478	–7834.689	–12.751	–37.038

[a] in kcal/mol

Table 4 — ADME results of related compounds

Parameters[a]	NIA1	NIA2	NIA3	NIA4	RV[b]
Stars	1	1	1	0	0-5
Amine	0	0	0	0	0-1
rtvFG	0	0	0	0	0-2
SASA	489.85	495.142	490.99	508.52	300.0-1000.0
FOSA	0	0	0	0	0.0-750.0
FISA	64.584	71.293	68.071	140.15	7.0-330.0
PISA	262.15	241.123	238.53	252.68	0.0-450.0
WPSA	163.116	182.725	184.38	115.68	0.0-175.0
donorHB	1	1	1	1	0.0-6.0
AccptHB	3.5	3.5	3.5	5	2.0-20.0
QPpolrz	27.419	27.387	27.327	27.635	13.0-70.0
QPPCaco	2417.97	2088.45	2240.7	464.34	<25 poor >500 great
QPlogBB	0.257	0.234	0.278	–0.653	–3.0- 1.2
QPPMDCK	10000	10000	10000	928.86	<25 poor >500 great
QPlogKp	–1.594	–1.792	–1.742	–2.924	–8.0 –1.0
metab	0	1	2	1	1-8
QPlogKhsa	0.069	0.078	0.078	–0.189	–1.5- 1.5
Percent Human-Oral Absorption	100	100	100	87.96	>80% is high <25% is poor
PSA	46.045	47.501	46.894	73.822	7.0- 200.0
RuleOfFive	0	0	0	0	Max is 4
RuleOfThree	0	0	0	0	Max is 3

[a] Stars: Number of property or descriptor values that fall outside the 95% range of similar values for known drugs; Amine: Number of non-conjugated amine groups; rtvFG: Number of reactive functional groups; SASA: Total solvent accessible surface area; FOSA: Hydrophobic component of the SASA; FISA: Hydrophilic component of the SASA; PISA: π (carbon and attached hydrogen) component of the SASA; WPSA: Weakly polar component of the SASA; donorHB: Estimated number of hydrogen bonds that would be donated; AccptHB: Estimated number of hydrogen bonds that would be accepted; QPpolrz: Predicted polarizability in cubic angstroms; QPPCaco: Predicted apparent Caco-2 cell permeability in nm/sec; QPlogBB: Predicted brain/blood partition coefficient; QPPMDCK: Predicted apparent MDCK cell permeability in nm/sec; QPlogKp: Predicted skin permeability; metab: Number of likely metabolic reactions; QPlogKhsa: Prediction of binding to human serum albumin; PercentHuman-OralAbsorption: Predicted human oral absorption on 0 to 100% scale; PSA: Van der Waals surface area of polar nitrogen and oxygen atoms; RuleOfFive: Number of violations of Lipinski's rule of five; RuleOfThree: Number of violations of Jorgensen's rule of three.

[b] RV: Recommended Value

the reference range are written in bold and it can be said that the most striking compound is NIA2. It is seen that NIA2 does not give results in terms of ADME property. When XTT results, molecular docking analysis and MM-GBSA results are considered in general, it can be said that NIA1 may be an effective candidate and further research should be carried out.

Pharmacophore Model

In the design of inhibitors, which are called small molecules, it is very important for the drug designer

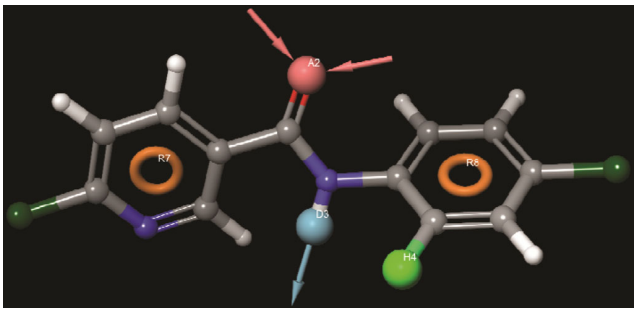

Fig. 6 — The pharmacophore map for studied compounds

to identify the main skeleton of the molecules that can interact and mark the regions where you can make changes without changing the main skeleton. For this goal, many pharmacophore model of studied compounds are calculated and the best most effective model is shown in Fig. 6.

Accoding to Fig. 6, there are 5 important region in the drug design processes. They are signed as A2, D3, H4 R7, and R8. These regions indicate that these regions must be present in the new molecules to be designed, and that it would also be appropriate to make the design by changing the remaining groups in the molecule. The region labeled A2 has a carbonyl group and is a suitable group for hydrogen bonding. This region is therefore labeled as acceptor region. The region labeled D3 has an amine group and can hydrogen bond using the hydrogen above it. This region is called the donor region. The region labeled H4 is the region required for hydrophobic interactions, while the regions labeled R7 and R8 are defined as the regions where aromatic rings should be present. As mentioned above, it is observed that designs should be made on the molecule without touching these regions.

Conclusion

In our study, four niacinamide compounds were synthesized. Spectral characterization of these compounds was done. Computational analyses were performed at B3LYP-D3/6-311++G(d,p) level in water. Obtained spectral results as experimentally were supported with the computational ones. Anticancer activity of newly synthesized compounds are investigated against colon, breast and gastric cancer cell line. NIA1 and NIA2 were found as active against gastric adenocarcinoma. *In silico* analyses were done in detail for the whole compounds. Molecular docking analyses were performed to predict anticancer and antibacterial properties. Furthermore, ADME and pharmacophore properties of these compounds were investigated. Finally, MM-GBSA analyses of complex structure in the result of molecular docking calculations were performed and binding energies were calculated. Considering all the results, it was observed that NIA1 and NIA2 showed effective results, with NIA1 being the better of the them.

Supplementary Information

Supplementary information is available in the website http://nopr.niscpr.res.in/handle/123456789/58776.

Acknowledgment

This research was made possible by TUBITAK ULAKBIM, High Performance, and Grid Computing Center (TR-Grid e-Infrastructure). This study was funded by the Scientific and Technological Research Council of Turkey (TUBITAK) BIDEB 2209A Grant No 1919 B012001929.

Conflict of interest

The authors declare no conflict of interest.

References

1 https://www.who.int/health-topics/cancer#tab=tab_1 – 21.07.2023.
2 Wu S, Huang Y, Zhang M, Gong Z, Wang G, Zheng X, Zong W, Zhao W, Xing P, Li R, Liu Z & Bao Y, *Nucleic Acids Res*, 51 (2023) D1196.
3 Schulz W A, *Molecular Biology of Human Cancers*, (Springer, Cham), 2023, p. 3–28.
4 Lashkarian M F, Hashemipour N, Niaraki N, Soghala S, Moradi A, Sarhangi S, Hatami M, Aghaei-Zarch F, Khosravifar M, Mohammedzadeh A, Najafi S, Majidpoor J, Farnia P & Aghaei-Zarch S M, *Can Cell Int*, 23 (2023) 29.
5 Abdelaziz A A S, Nawaz M, Izzeldin I, Abubshait H A, Alsadig A, Gomaa M S, Abubshait S A & Alsewdan D, *J Mol Struc*, 1275 (2023) 134702.
6 Mandour H S A, Hamed M A, Saad-Allah K M, Abd Elnabi M K, Abosharaf H A & El-Gharably A A, *Chem Sel*, 8 (2023) e202300254.
7 Ashok D, Thara G, Kumar B K, Srinivas G, Ravinder D, Vishnu T, Sarasija M & Sushmitha B, *RSC Adv*, 13 (2023) 25.
8 Puri S, Ahmad I, Patel H, Kumar K & Juvale K, *Toxic Vitro*, 86 (2023) 105517.
9 Patel K B, Mukherjee S, Bhatt H, Rajani D, Ahmad I, Patel H & Kumari P, *J Mol Struc*, 1276 (2023) 134755.
10 Çapan I, Hawash M, Jaradat N, Sert Y, Servi R & Koca I, *BMC Chem*, 17 (2023) 60.
11 Majewski G P, *J Clin Dermatol Ther*, 9 (2023) 119.
12 Wu W, Yuan S, Tang Y, Meng X, Peng M, Hu Z & Liu W, *Nutrients*, 15 (2023) 2851.
13 Mourelle M L, Gomez C P & Legido J L, *Appl Sci*, 13 (2023) 850.
14 To C, Beyett T S, Jang J, Feng W W, Bahcall M, Haikala H M, Shin B H, Heppner D E, Rana J K, Leeper B A, Soroko K M,

Poitras M J, Gokhale P C, Kobayashi Y, Wahid K, Kurppa K J, Gero T W, Cameron M D, Ogino A, Mushajiang M, Xu C, Zhang Y, Scott D A, Eck M J, Gray N S & Janne P A, *Nat Cancer*, 3 (2022) 402.

15 Olivier N B, *J Med Chem*, 57 (2014) 4584.

16 Taşkın K A H, Tüzün G, Güney E, Aslan R, Sayin K, Tüzün B & Ataseven H, *Struc Chem*, 33 (2022) 1189.

17 Gauss View, Version 6.1, Roy Dennington, Keith T A & Millam J M, Semichem Inc, Shawnee Mission, KS, (2016)

18 Gaussian 16, Revision B.01, Frisch M J, Trucks G W, Schlegel H B, G E Scuseria, M A Robb, J R Cheeseman, G Scalmani, V Barone, G A Petersson, H Nakatsuji, X Li, M Caricato, A V Marenich, J Bloino, B G Janesko, R Gomperts, B Mennucci, H P Hratchian, J V Ortiz, A F Izmaylov, J L Sonnenberg, D Williams-Young, F Ding, F Lipparini, F Egidi, J Goings, B Peng, A Petrone, T Henderson, D Ranasinghe, V G Zakrzewski, J Gao, N Rega, G Zheng, W Liang, M Hada, M Ehara, K Toyota, R Fukuda, J Hasegawa, M Ishida, T Nakajima, Y Honda, O Kitao, H Nakai, T Vreven, K Throssell, J A Montgomery, J E Peralta, F Ogliaro, M J Bearpark, J J Heyd, E N Brothers, K N Kudin, V N Staroverov, T A Keith, R Kobayashi, J Normand, K Raghavachari, A P Rendell, J C Burant, S S Iyengar, J Tomasi, M Cossi, J M Millam, M Klene, C Adamo, R Cammi, J W Ochterski, R L Martin, K Morokuma, O Farkas, J B Foresman & D J Fox, (Gaussian, Inc., Wallingford CT), 2016.

19 Maestro Version 12.8.117, MMshare Version 5.4.117, Release 2021-2, Platform Windows-x64, Schrödinger.

20 Feng X, Wang Y & Xu L, *Gastroenterol Hepatol Res*, 4 (2022) 2.

21 *Schrödinger Release 2021-2: LigPrep*, (Schrödinger, LLC, New York) 2021.

22 A) Schrödinger Release 2021-2: Protein Preparation Wizard; Epik, (Schrödinger, LLC, New York), 2021; B) Impact, Schrödinger, LLC, New York, NY; Prime, (Schrödinger, LLC, New York), 2021.

23 A) Schrödinger Release 2021-2: QM-Polarized Ligand Docking protocol; Glide, (Schrödinger, LLC, New York), 2021; B) Jaguar, (Schrödinger, LLC, New York), 2021; C) QSite, (Schrödinger, LLC, New York), 2021.

24 Schrödinger Release 2021-2: QikProp, (Schrödinger, LLC, New York), 2021.

25 Schrödinger Release 2021-2: Phase, (Schrödinger, LLC, New York), 2021.